Competing orders in Na_xCoO_2 from strong correlations on a two-particle level

Lewin Boehnke and Frank Lechermann
I. Institut für Theoretische Physik, Universität Hamburg, D-20355 Hamburg, Germany
(Received 17 January 2011; published 28 March 2012)

Based on dynamical mean-field theory with a continuous-time quantum Monte Carlo impurity solver, static as well as dynamic spin and charge susceptibilites for the phase diagram of the sodium cobaltate system Na_xCoO_2 are discussed. The approach includes important vertex contributions to the **q** dependent two-particle response functions by means of a local approximation to the irreducible vertex function in the particle-hole channel. A single-band Hubbard model suffices to reveal several charge- and spin-instability tendencies in accordance with experiment, including the stabilization of an effective kagome sublattice close to $x = 0.67$, without invoking the doping-dependent Na-potential landscape. The in-plane antiferromagnetic-to-ferromagnetic crossover is additionally verified by means of the computed Korringa ratio. Moreover an intricate high-energy mode in the transverse spin susceptiblity is revealed, pointing toward a strong energy dependence of the effective intersite exchange.

DOI: 10.1103/PhysRevB.85.115128 PACS number(s): 71.27.+a, 71.10.Fd, 71.30.+h, 75.30.Cr

I. INTRODUCTION

The investigation of finite-temperature phase diagrams of realistic strongly correlated systems is a quite formidable task due to the often tight competition between various low-energy ordering instabilities. In this respect the quasi-two-dimensional (quasi-2D) sodium cobaltate system Na_xCoO_2 serves as a notably challenging case.[1,2] Here $x \in [0,1]$ nominally mediates between the $Co^{4+}(3d^5, S = \frac{1}{2})$ and $Co^{3+}(3d^6, S = 0)$ low-spin states. Thus the Na ions provide the electron doping for the nearly filled t_{2g} states of the triangular CoO_2 layers up to the band-insulating limit $x = 1$. Coulomb correlations with a Hubbard U up to 5 eV for the t_{2g} manifold of bandwidth $W \sim 1.5$ eV[3] are revealed from photoemission.[4] Hence with $U/W \gg 1$ the frustrated metallic system is definitely placed in the strongly correlated regime.

Various different electronic phases and regions for temperature T versus doping x are displayed in the experimental sodium cobaltate phase diagram (see Fig. 1), for instance, a superconducting dome ($T_c \sim 4.5$ K) stabilized by intercalation with water close to $x = 0.3$.[5] Pauli-like magnetic susceptibility is found in the range $x < 0.5$[1] with evidence for 2D antiferromagnetic (AFM) correlations.[2,6] For $x > 0.5$, spin fluctuations and increased magnetic response show up for $0.6 < x < 0.67$, including the evolution to Curie-Weiss (CW) behavior[1] for $0.6 < x < 0.75$ and the eventual onset of in-plane ferromagnetic (FM) order. The ordered magnetic structure in the doping range $0.75 < x < 0.9$ with $T_N \sim 19$–27 K[7–10] is of A-type AFM for the FM CoO_2 layers. As the local spin-density approximation (LSDA) is not sufficient to account for the AFM-to-FM crossover with x,[3] explicit many-body approaches are needed.[11–13]

Several theoretical works have dealt with the influence of the sodium arrangements on the electronic properties of Na_xCoO_2, both from the viewpoint of disordered sodium ions[12] as well as from orderings for certain dopings.[14–16] However, whether such sodium patterns are due to sole (effective) single-particle potentials or mainly originating from many-body effects within the CoO_2 planes is still a matter of debate.[17,18]

In this paper, we report the fact that a large part of the electronic (spin and charge) phase diagram of sodium cobaltate may be well described within a Hubbard model using realistic dispersions and without invoking the details of the sodium arrangement. Therefore most of the observed crossovers and instabilities are truly driven by strong correlation effects and can scarcely be described by a weak-coupling expansion around the noninteracting case. The theoretical study is elucidating the two-particle correlations in the particle-hole channel computed within dynamical mean-field theory (DMFT) including vertex contributions (for a review, see, e.g., Refs. 19 and 20). So far the latter have been neglected in cobaltate susceptibilities based on LSDA[21,22] and the fluctuation-exchange approximation.[22,23] Our dynamical lattice susceptibilities allow us to reveal details of the AFM-to-FM crossover with T and of the intriguing charge-ordering tendencies, both in line with recent experimental data.[2,24] Moreover, insight in the $(x, \mathbf{q})$ dependent spin excitations at finite frequency is provided.

II. MODELING AND METHOD

Since we are mainly interested in the $x > 0.5$ part of the phase diagram, the low-energy band dispersion of sodium cobaltate is described within an a_{1g}-like single-band approach, justified from photoemission[25] and Compton scattering[26] experiments. We primarily focus on the in-plane processes on the effective triangular Co lattice with tight-binding parameters up to the third-nearest-neighbor (NN) hopping, i.e., $(t, t', t'') = (-202,\ 35,\ 29)$ meV[27] for the 2D dispersion. Although intersite Coulomb interactions might play a role,[13] the canonical modeling was restricted to an on-site Coulomb interaction $U = 5$ eV. Our calculations show that already substantial nonlocal correlations originate therefrom. The resulting Hubbard model on the triangular lattice is solved within DMFT for the local one-particle Green's function $G(\tau_{12}) = -\langle T_\tau c(\tau_1) c^\dagger(\tau_2)\rangle$ with $\tau_{uv} = \tau_u - \tau_v$ and T_τ being the time-ordering operator. The DMFT problem is approached with the continuous-time quantum Monte Carlo methodology[28,29] in its hybridization-expansion flavor[29] as implemented in the TRIQS package.[30] Additionally we implemented the computation of the impurity two-particle Green's function[31] $G^{(2)}(\tau_{12}, \tau_{34}, \tau_{14}) = -\langle T_\tau c^\dagger(\tau_1) c(\tau_2) c^\dagger(\tau_3) c(\tau_4)\rangle$ to address explicit electron-electron correlations. In the approximation of a purely local particle-hole irreducible vertex,

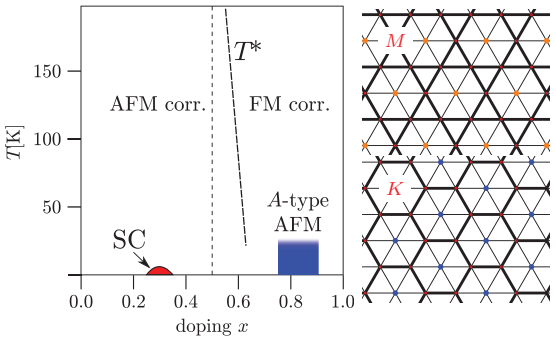

FIG. 1. (Color online) Left: Sketched Na_xCoO_2 diagram of dominating correlations and stable phases, based on Ref. 2. Right: M point ordering (top) and K point ordering (bottom) on the triangular lattice separating the lattice into a triangular sublattice (squares) and a kagome, honeycomb sublattice (thick lines).

$G^{(2)}$ allows us to also determine lattice susceptibilities.[19,20,31,32] These susceptibilities, e.g., for spin (s) and charge (c), written as

$$\chi_{s/c}(i\omega,\mathbf{q},T) = T^2 \sum_{\nu\nu'} \left(\tilde{\chi}^{(0)}_{s/c,\nu\nu'}(i\omega,\mathbf{q},T) + v_{s/c,\nu\nu'}(i\omega,\mathbf{q},T)\right), \tag{1}$$

where ω (ν) marks bosonic (fermionic) Matsubara frequencies, consist of two parts. Namely $\tilde{\chi}^{(0)}_{s/c,\nu\nu'}$ denotes the conventional (Lindhard-like) term, built up from the (renormalized) bubble part, which is mainly capable of detecting Fermi-surface-driven instabilities close to $T = 0$, but the second part $v_{s/c,\nu\nu'}$ (the vertex term) includes properly the energy dependence of the response behavior due to strong local interactions in real space. It proves important for revealing, e.g., magnetic instabilities at finite T due to the resolution of the two-particle correlations governed by an implicit intersite exchange J. Note that all numerics take advantage of the recently introduced orthogonal polynomial representation[31] of one- and two-particle Green's functions to provide the needed high accuracy and to eliminate artifacts often stemming from truncating the Fourier-transformed $G^{(2)}$ in Matsubara space.

Within the first Brillouin zone (BZ) of the triangular coordination with lattice constant a, the coherent Γ point instability signals FM order in the case of χ_s and phase separation for χ_c. Additionally important here are the instabilities at the the K and M points. The associated orderings give rise to distinct sublattice structures in real space (cf. Fig. 1). The M point ordering leads to a triangular and a kagome sublattice with lattice constant $a_{\text{eff}} = 2a$, while the K point ordering establishes a triangular and a honeycomb sublattice with $a_{\text{eff}} = \sqrt{3}a$, respectively.

III. RESULTS

A. Static properties

We will first discuss the static $[\chi_{s/c}(\omega = 0,\mathbf{q},T)]$ response (read off from the zeroth bosonic Matsubara frequency), directly reflecting the system's susceptibility to an order of the ($\mathbf{q}$-resolved) type. The cobaltate intralayer charge susceptibility $\chi_c(0,\mathbf{q},T)$ shows pronounced features in $\mathbf{q}$ space with doping x (see Fig. 2). Close to $x = 0.3$ our single-band modeling leads to increased intensity inside the BZ, pointing toward longer-range charge-modulation (e.g., 3×3, etc.) tendencies in real space. That $Na_{1/3}CoO_2$ is indeed prone to such 120°-like instabilities has been experimentally suggested by Qian *et al.*[33] Toward $x = 0.5$ the susceptibility for short-range charge modulation grows in χ_c, displaying a diffuse high-intensity distribution at the BZ edge with a maximum at the K point for $x = 0.5$. No detailed conclusive result on the degree and type of charge ordering for the latter composition is known from experiments; however, chainlike charge disproportionation that breaks the triangular symmetry has been verified.[34,35] The present single-site approach cannot stabilize such symmetry breakings, but a pronounced χ_c at the K point at least inherits some stripelike separation of the two involved sublattices. Near $x = 0.67$, the χ_c maximum has shifted to the M point, in line with the detection of an effective kagome lattice from nuclear magnetic resonance (NMR) experiments.[24] For even higher doping, this $\mathbf{q}$ dependent structuring transmutes into a Γ point maximum, pointing toward known phase-separating tendencies.[36] Figure 2 also exhibits the x dependent intralayer spin susceptibility, starting with strong AFM peaks at $x = 0.3$ due to K point correlations. With reduced intensity these shift to the M point at $x = 0.5$, consistent with different types of spin and charge orderings at this doping level.[35] For $x > 0.5$, $\chi_s(\mathbf{q},T,0)$ first develops broad intensity over the full BZ before forming a pronounced peak at the Γ point above $x \sim 0.6$. Thus the experimentally observed crossover of the in-plane AFM-to-FM tendencies in the spin response is reproduced.

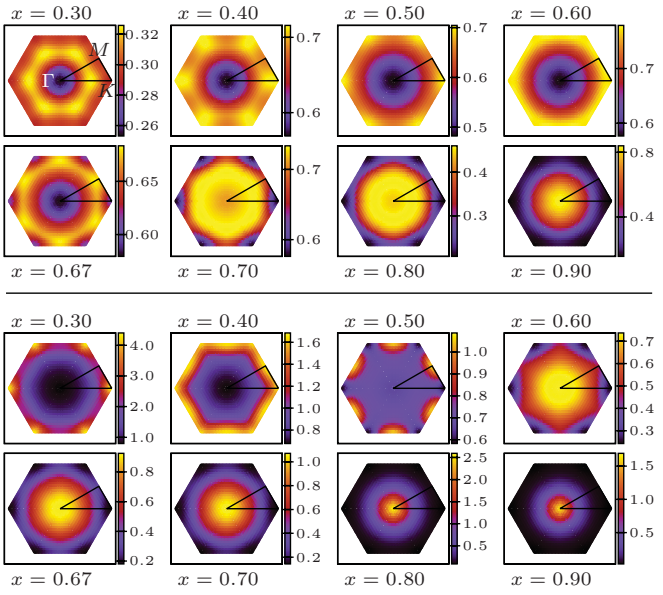

FIG. 2. (Color online) Static in-plane charge (top) and spin (bottom) susceptibility $\chi(0,\mathbf{q},T)$ with doping at $T = 386$ K.

Lang *et al.*[2] revealed from the Na NMR that this crossover is T dependent with x, resulting in an energy scale T^* below which AFM correlations are favored (cf. Fig. 1). The slope $\partial T^*/\partial x$ turns out negative, in line with the general argument that FM correlations are most often favored at elevated T because of the entropy gain via increased transverse

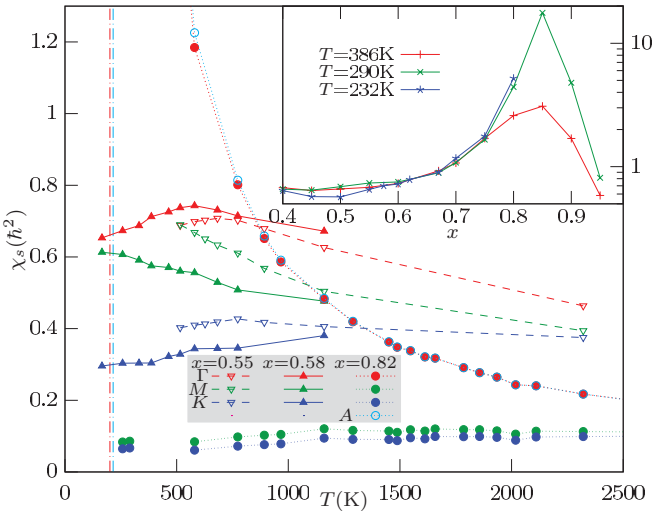

FIG. 3. (Color online) Temperature dependence of the spin susceptibility at the Γ, M, and K point for $x = 0.55$, 0.58, and 0.82. For the latter, values at the A point are also included. Vertical lines indicate extrapolated transition temperatures for Γ (FM) spin ordering and A (A-type AFM) spin ordering respectively for $x = 0.82$. The inset shows the doping dependence of the uniform ($\mathbf{q} = \Gamma$) in-plane spin susceptibility χ_s for various T. Note the largely increased magnitude of χ_s for $x \geqslant 0.75$ in this log-scale plot.

spin fluctuations. In this respect, Fig. 3 shows the $(x,T,\mathbf{q})$ dependence of the computed χ_s. For $x = 0.55$, 0.58, a maximum in the Γ point susceptibility is revealed, which has been interpreted by Lang *et al.*[2] as the criterion for a change in the correlation characteristics, thereby defining the T^* line. While the temperature scale exceeds the experimental value in the present mean-field formalism, the qualitatively correct doping behavior of the T^* line is obtained.

Beyond the experimental findings our calculations allow us to further investigate the nature of the magnetic crossover. Figure 3 reveals that at lower T and x closer to $x = 0.5$ the susceptibility at Γ is ousted by the one at M, while χ_s at K is mostly dispensable. The M susceptibility can be understood due to the proximity of the striped order at $x = 0.5$,[1,17,37] which is, however, not realized until much lower temperatures.

The inset of Fig. 3 follows the T dependent Γ point susceptibility through a vast doping range. Note the subtle resolution around $x = 0.5$ as well as the large exaggeration, especially for lower temperatures in the experimentally verified in-plane FM region. The main panel of Fig. 3 additionally shows for $x = 0.82$ the spin susceptibility at the A point [i.e., at $k_z = (0,0,\frac{1}{2})$ in the BZ), which denotes the A-type AFM order. While Γ and A show CW behavior, the extrapolated transition temperature is ∼7% higher at A than at Γ, verifying the experimental findings of A-type order.[7–10] In the temperature scan we additionally introduced a nearest-layer interplane hopping $t_\perp = 13$ meV;[9,13,38] however, the previous in-plane results are qualitatively not affected by this model extension. Due to known charge disproportionation the inclusion of long-range Coulomb interactions, e.g., via an intersite V,[13,16] seems reasonable. This was abandoned in the present single-site DMFT approach, resulting generally in reduced charge response. Without V, charge fluctuations are substantially suppressed for large U/W, while the intersite spin fluctuations are still strong due to superexchange.

B. Dynamical properties

Aside from the static response, our method allows access to the dynamic regime. Figure 4 shows the dynamical transverse spin susceptibility for fixed $T = 580$ K for selected x. Note the broad $\mathbf{q}$ dependence and small excitation energy in the low-doping regime. In contrast, the FM correlations near $x = 0.82$ are reflected by strong paramagnon-like gapless excitation at Γ combined with very little weight and rather high excitation energies at AFM wave vectors. Interestingly, a comparably strong and sharp K-type high-energy excitation (∼1 eV) for larger x below the onset of in-plane FM order is revealed. Its amplitude is strongest at $x = 0.67$ while its energy increases with x and it is worthwhile to note that the mode is *neither* visible when neglecting vertex contributions *nor* in a plain triangular Hubbard model with NN hopping only. Thus it reflects a strong energy dependence of the intersite exchange coupling $J = J(x,\mathbf{q},\omega)$ that obviously changes character for $x \sim 0.67$ with $\mathbf{q}$ and ω. The predicted high-energy feature could be probed experimentally and also studied in time-dependent measurements. We propose the use of modern laser-pulse techniques[39] to address this problem.

Experimentally, the evidence for significant $\mathbf{q} \neq 0$ fluctuations is drawn[2,40] from the Korringa ratio[41–44]

$$\mathcal{K}_x^T = \frac{\hbar}{4\pi k_B}\left(\frac{\gamma_e}{\gamma_N}\right)^2 \frac{1}{T_1 T K_S^2},$$
$$\frac{1}{T_1 T} = \lim_{\omega\to 0} \frac{2k_B}{\hbar^2} \sum_{\mathbf{q}} |A(\mathbf{q})|^2 \frac{\Im\chi_s^{-+}(\omega,\mathbf{q},T)}{\omega}, \qquad (2)$$
$$K_S = \frac{|A(\mathbf{0})|\gamma_e \Re\chi_s^{-+}(0,\mathbf{0},T)}{\gamma_N \hbar^2},$$

where $1/T_1$ is the nuclear relaxation rate, K_S is the NMR field shift, γ_e (γ_N) is the electronic (nuclear) gyromagnetic ratio, $A(\mathbf{q})$ is the hyperfine coupling, and k_B is the Boltzmann constant. $\Re\chi_s^{-+}$ and $\Im\chi_s^{-+}$ denote the real and imaginary parts of the transverse spin susceptibility, respectively. Roughly speaking, $\mathcal{K} > 1$ signals AFM correlations, $\mathcal{K} < 1$ points to FM tendencies in χ_s, and the term "Korringa behavior"

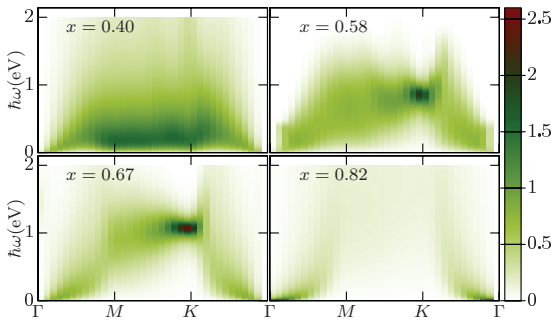

FIG. 4. (Color online) Imaginary part of the dynamical spin susceptibility for $T = 580$ K for selected dopings.

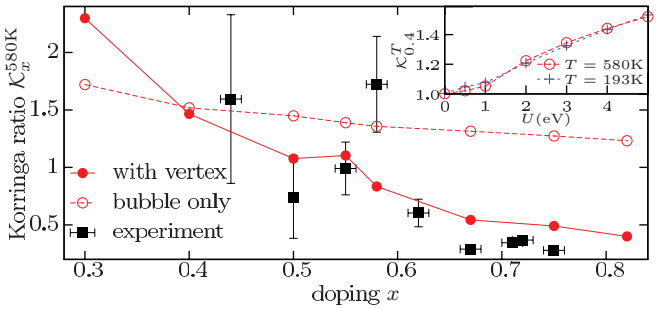

FIG. 5. (Color online) Korringa ratio versus doping for $T = 580$ K. The experimental data, extracted from Refs. 40 and 2, were obtained for lower temperatures. The inset shows the evolution of the bubble-diagram contribution from the analytically known value $\mathcal{K} = 1$ for the noninteracting ($U = 0$) case[41] to the fully interacting ($U = 5$ eV) calculation.

generally denotes the regime $\mathcal{K}(T) \sim 1$. In single-atom unit cells, $A(\mathbf{q})$ becomes $\mathbf{q}$ independent.

Note that $1/T_1$ especially is numerically expensive, as it requires calculation of χ_s^{-+} on many Matsubara frequencies with subsequent analytical continuation to the real frequency axis for contributions beyond the bubble diagram. Figure 5 finally shows the AFM-to-FM correlation crossover captured by the Korringa ratio over a wide doping range. The overall agreement with experimental results is conclusive. Relevant deviations in the low-doping regime probably originate from the smaller temperatures studied in the experiment. The difference at $x = 0.58$ might be of the same origin, but since charge ordering occurs for $x > 0.5$, which was not included explicitly here, neglecting the $\mathbf{q}$ dependence of $A(\mathbf{q})$ might be also questionable.[45] One can see that the bubble-only calculation yields a nearly flat Korringa ratio with doping and thus fails completely in explaining the experimental findings. In particular it does not reflect the strong FM correlations for high doping. This further proves the importance of strong correlations on the two-particle level, asking for substantial vertex contributions.[43] Note that the recently suggested lower-energy effective kagome model[16] including the effect of charge ordering is not contradicting the present modeling, since here the effective kagome lattice naturally shows up and also the key properties of the spin degrees of freedom seem well described on the original triangular lattice.

IV. CONCLUSION

In summary, the DMFT computation of two-particle observables including vertex contributions based on a realistic single-band Hubbard modeling for Na_xCoO_2 leads to a faithful phase-diagram examination at larger x, including the kagome-like charge-ordering tendency for $x \sim 0.67$ and the in-plane AFM-to-FM crossover associated with a temperature scale T^*. Thus it appears that many generic cobaltate features are already governed by a canonical correlated model, without invoking the details of the doping-dependent sodium-potential landscape or the inclusion of multiorbital processes. Of course, future work has to concentrate on quantifying further details of the various competing instabilities (and their mutual couplings) within extended model considerations. Beyond equilibrium physics, we predict a strong energy dependence of the effective intersite exchange resulting in an K-type high-energy mode around $x = 0.67$, which could be probed in experimental studies.

ACKNOWLEDGMENTS

The authors are indebted to O. Parcollet and M. Ferrero for useful discussions on the vertex implementation and calculation. We also thank A. Georges, H. Hafermann, A. I. Lichtenstein, O. Peil, and C. Piefke for valuable comments. This work was supported by the SPP 1386, the FOR 1346, and the SFB925 of the DFG. Computations were performed at the North-German Supercomputing Alliance (HLRN) and the regional computing center (RRZ) of the University of Hamburg.

[1] M. L. Foo, Y. Wang, S. Watauchi, H. W. Zandbergen, T. He, R. J. Cava, and N. P. Ong, Phys. Rev. Lett. **92**, 247001 (2004).
[2] G. Lang, J. Bobroff, H. Alloul, G. Collin, and N. Blanchard, Phys. Rev. B **78**, 155116 (2008).
[3] D. J. Singh, Phys. Rev. B **61**, 13397 (2000).
[4] M. Z. Hasan, Y.-D. Chuang, D. Qian, Y. W. Li, Y. Kong, A. P. Kuprin, A. V. Fedorov, R. Kimmerling, E. Rotenberg, K. Rossnagel, Z. Hussain, H. Koh, N. S. Rogado, M. L. Foo, and R. J. Cava, Phys. Rev. Lett. **92**, 246402 (2004).
[5] K. Takada, H. Sakurai, E. Takayama-Muromachi, F. Izumi, R. A. Dilanian, and T. Sasaki, Nature (London) **422**, 53 (2003).
[6] T. Fujimoto, G.-Q. Zheng, Y. Kitaoka, R. L. Meng, J. Cmaidalka, and C. W. Chu, Phys. Rev. Lett. **92**, 047004 (2004).
[7] J. Sugiyama, H. Itahara, J. H. Brewer, E. J. Ansaldo, T. Motohashi, M. Karppinen, and H. Yamauchi, Phys. Rev. B **67**, 214420 (2003).
[8] A. T. Boothroyd, R. Coldea, D. A. Tennant, D. Prabhakaran, L. M. Helme, and C. D. Frost, Phys. Rev. Lett. **92**, 197201 (2004).
[9] S. P. Bayrakci, I. Mirebeau, P. Bourges, Y. Sidis, M. Enderle, J. Mesot, D. P. Chen, C. T. Lin, and B. Keimer, Phys. Rev. Lett. **94**, 157205 (2005).
[10] P. Mendels, D. Bono, J. Bobroff, G. Collin, D. Colson, N. Blanchard, H. Alloul, I. Mukhamedshin, F. Bert, A. Amato, and A. D. Hillier, Phys. Rev. Lett. **94**, 136403 (2005).
[11] J. O. Haerter, M. R. Peterson, and B. S. Shastry, Phys. Rev. Lett. **97**, 226402 (2006).
[12] C. A. Marianetti and G. Kotliar, Phys. Rev. Lett. **98**, 176405 (2007).
[13] C. Piefke, L. Boehnke, A. Georges, and F. Lechermann, Phys. Rev. B **82**, 165118 (2010).
[14] J. Merino, R. H. McKenzie, and B. J. Powell, Phys. Rev. B **80**, 045116 (2009).
[15] S. Zhou and Z. Wang, Phys. Rev. Lett. **98**, 226402 (2007).
[16] O. E. Peil, A. Georges, and F. Lechermann, Phys. Rev. Lett. **107**, 236404 (2011).

[17]H. W. Zandbergen, M. L. Foo, Q. Xu, V. Kumar, and R. J. Cava, Phys. Rev. B **70**, 024101 (2004).
[18]Y. Hinuma, Y. S. Meng, and G. Ceder, Phys. Rev. B **77**, 224111 (2008).
[19]A. Georges, G. Kotliar, W. Krauth, and M. J. Rozenberg, Rev. Mod. Phys. **68**, 13 (1996).
[20]T. Maier, M. Jarrell, T. Pruschke, and M. H. Hettler, Rev. Mod. Phys. **77**, 1027 (2005).
[21]M. D. Johannes, I. I. Mazin, D. J. Singh, and D. A. Papaconstantopoulos, Phys. Rev. Lett. **93**, 097005 (2004).
[22]M. M. Korshunov, I. Eremin, A. Shorikov, V. I. Anisimov, M. Renner, and W. Brenig, Phys. Rev. B **75**, 094511 (2007).
[23]K. Kuroki, S. Onari, Y. Tanaka, R. Arita, and T. Nojima, Phys. Rev. B **73**, 184503 (2006).
[24]H. Alloul, I. R. Mukhamedishin, T. A. Platova, and A. V. Dooglav, Europhys. Lett. **85**, 47006 (2009).
[25]D. Qian, L. Wray, D. Hsieh, L. Viciu, R. J. Cava, J. L. Luo, D. Wu, N. L. Wang, and M. Z. Hasan, Phys. Rev. Lett. **97**, 186405 (2006).
[26]J. Laverock, S. B. Dugdale, J. A. Duffy, J. Wooldridge, G. Balakrishnan, M. R. Lees, G.-Q. Zheng, D. Chen, C. T. Lin, A. Andrejczuk, M. Itou, and Y. Sakurai, Phys. Rev. B **76**, 052509 (2007).
[27]H. Rosner, S.-L. Drechsler, G. Fuchs, A. Handstein, A. Wälte, and K.-H. Müller, Braz. J. Phys. **33**, 718 (2003).
[28]A. N. Rubtsov, V. V. Savkin, and A. I. Lichtenstein, Phys. Rev. B **72**, 035122 (2005).
[29]P. Werner, A. Comanac, L. de' Medici, M. Troyer, and A. J. Millis, Phys. Rev. Lett. **97**, 076405 (2006).
[30]M. Ferrero and O. Parcollet (unpublished).
[31]L. Boehnke, H. Hafermann, M. Ferrero, F. Lechermann, and O. Parcollet, Phys. Rev. B **84**, 075145 (2011).
[32]V. Zlatić and B. Horvatić, Solid State Commun. **75**, 263 (1990).
[33]D. Qian, D. Hsieh, L. Wray, Y.-D. Chuang, A. Fedorov, D. Wu, J. L. Lue, N. L. Wang, L. Viciu, R. J. Cava, and M. Z. Hasan, Phys. Rev. Lett. **96**, 216405 (2006).
[34]Q. Huang, M. L. Foo, J. W. Lynn, H. W. Zandbergen, G. Lawes, Y. Wang, B. H. Toby, A. P. Ramirez, N. P. Ong, and R. J. Cava, J. Phys.: Condens. Matter **16**, 5803 (2004).
[35]F. L. Ning, S. M. Golin, K. Ahilan, T. Imai, G. J. Shu, and F. C. Chou, Phys. Rev. Lett. **100**, 086405 (2008).
[36]M. Lee, L. Viciu, L. Li, Y. Wang, M. L. Foo, S. Watauchi, R. A. Pascal, R. J. Cava, and N. P. Ong, Nat. Mater. **5**, 537 (2006).
[37]G. Gašparović, R. A. Ott, J.-H. Cho, F. C. Chou, Y. Chu, J. W. Lynn, and Y. S. Lee, Phys. Rev. Lett. **96**, 046403 (2006).
[38]C. Fouassier, G. Matejka, J.-M. Reau, and P. Hagenmuller, J. Solid State Chem. **6**, 532 (1973).
[39]A. V. Kimel, C. D. Stanciu, P. A. Usachev, R. V. Pisarev, V. N. Gridnev, A. Kirilyuk, and T. Rasing, Phys. Rev. B **74**, 060403(R) (2006).
[40]H. Alloul, I. R. Mukhamedshin, G. Collin, and N. Blanchard, Europhys. Lett. **82**, 17002 (2008).
[41]J. Korringa, Physica (Amsterdam) **16**, 601 (1950).
[42]T. Moriya, J. Phys. Soc. Jpn. **18**, 516 (1963).
[43]E. Yusuf, B. J. Powell, and R. H. McKenzie, J. Phys.: Condens. Matter **21**, 195601 (2009).
[44]Note that we use a slightly different definition of χ_s than Ref. 43.
[45]A further reason could be an additional peak in the corresponding measurement at this precise doping,[2] which may or may not be of electronic nature, possibly influencing the Korringa ratio.